Electronic Supplementary Material (ESI) for Journal of Materials Chemistry A.

Supporting Information

Synergistic effect of cooperating solvent vapor annealing for high-efficiency planar inverted perovskite solar cells

Ahra Yi[†], Sangmin Chae[†], Hanbin Lee, Hyo Jung Kim[*]

Supporting Information

Title

Synergistic effect of cooperating solvent vapor annealing for high-efficiency planar inverted perovskite solar cells

*Ahra Yi †, Sangmin Chae†, Hanbin Lee, Hyo Jung Kim**

Department of Organic Material Science and Engineering, Pusan National University, Busan, South Korea

† These authors are equally contributed to this work.

E-mail to: hyojkim@pusan.ac.kr

Contents

All measured spectra were corrected to 284.8 eV according to the C 1s binding energy for aliphatic carbon and the fitting was performed using the Gaussian-Lorentzian function.

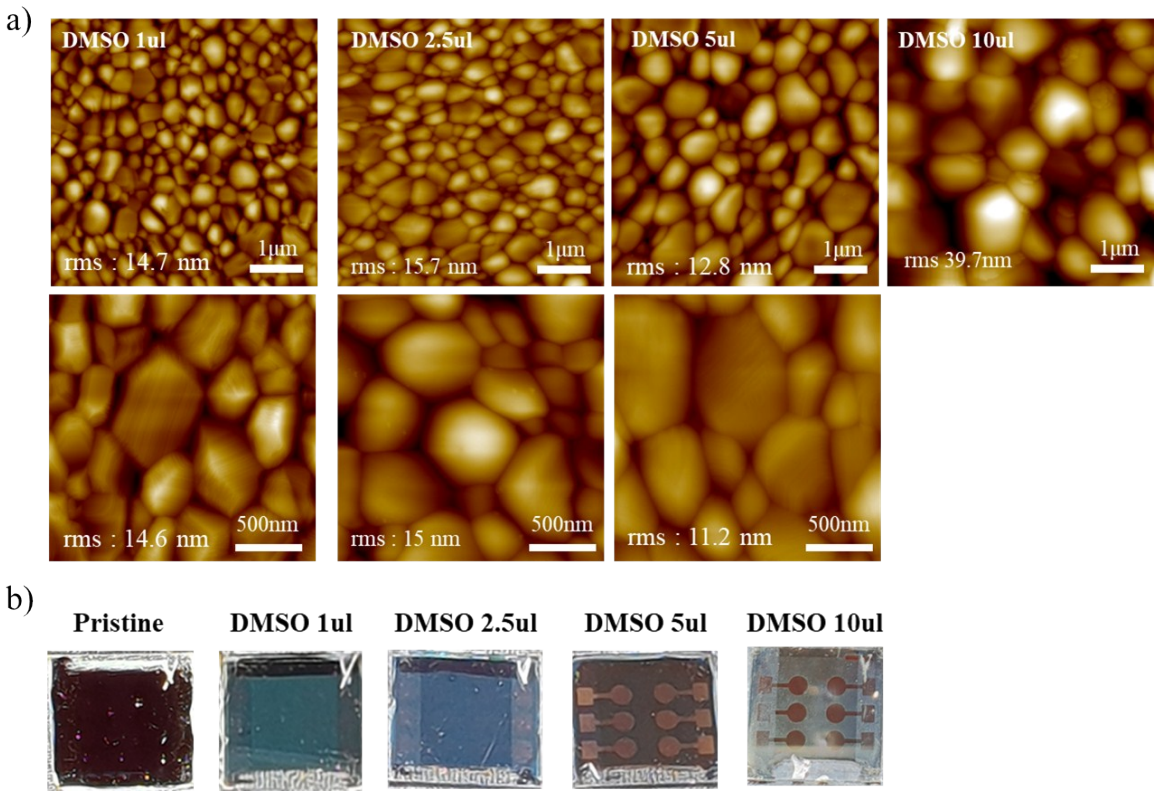

Figure S1 a) The atomic force microscopy (AFM) and b) device images using various amount of DMSO solvent.

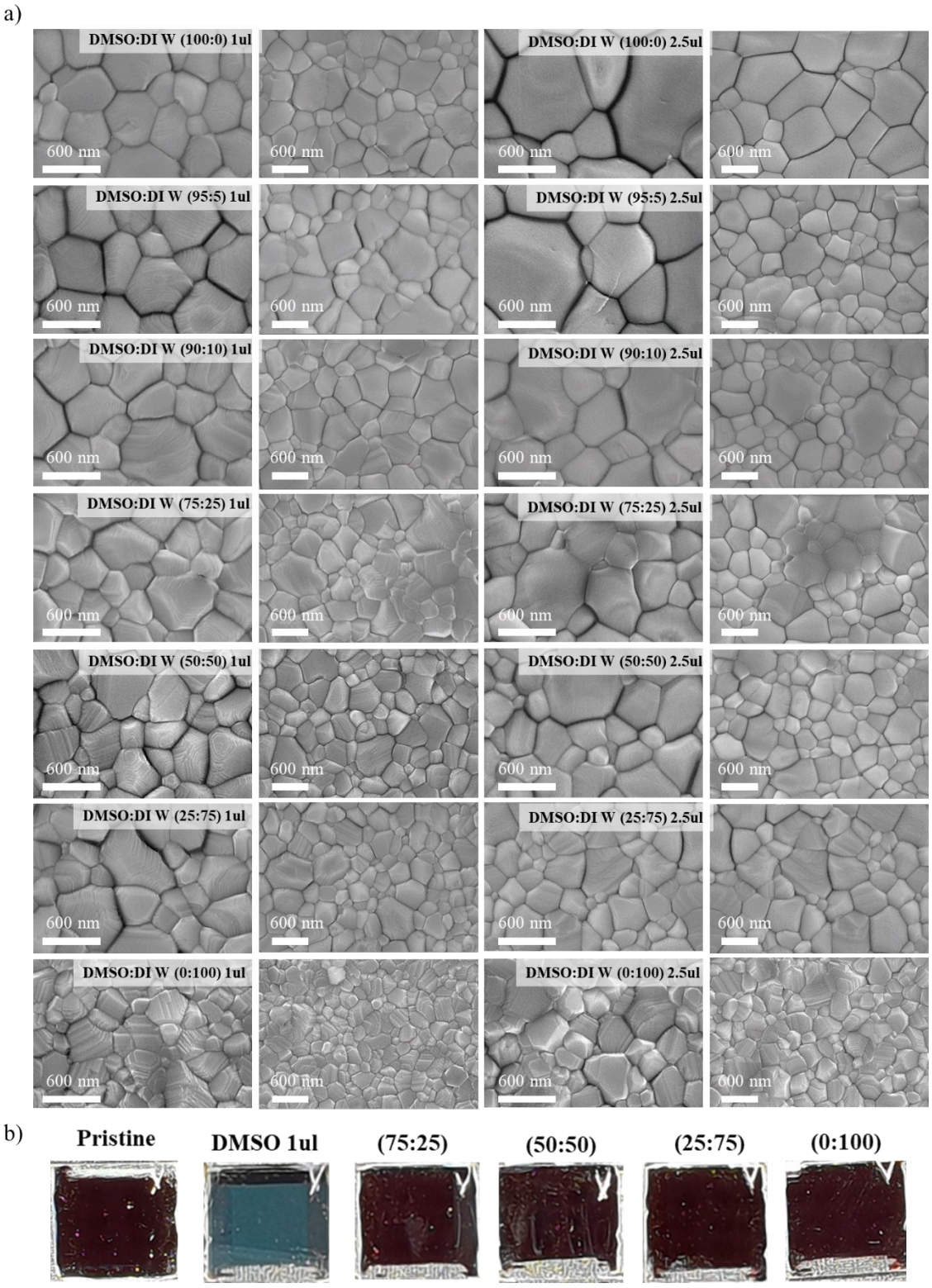

Figure S2 a) The scanning electron microscopy (SEM) and b) device images of an optimization process using various ratio of DMSO:DI water 1 uL.

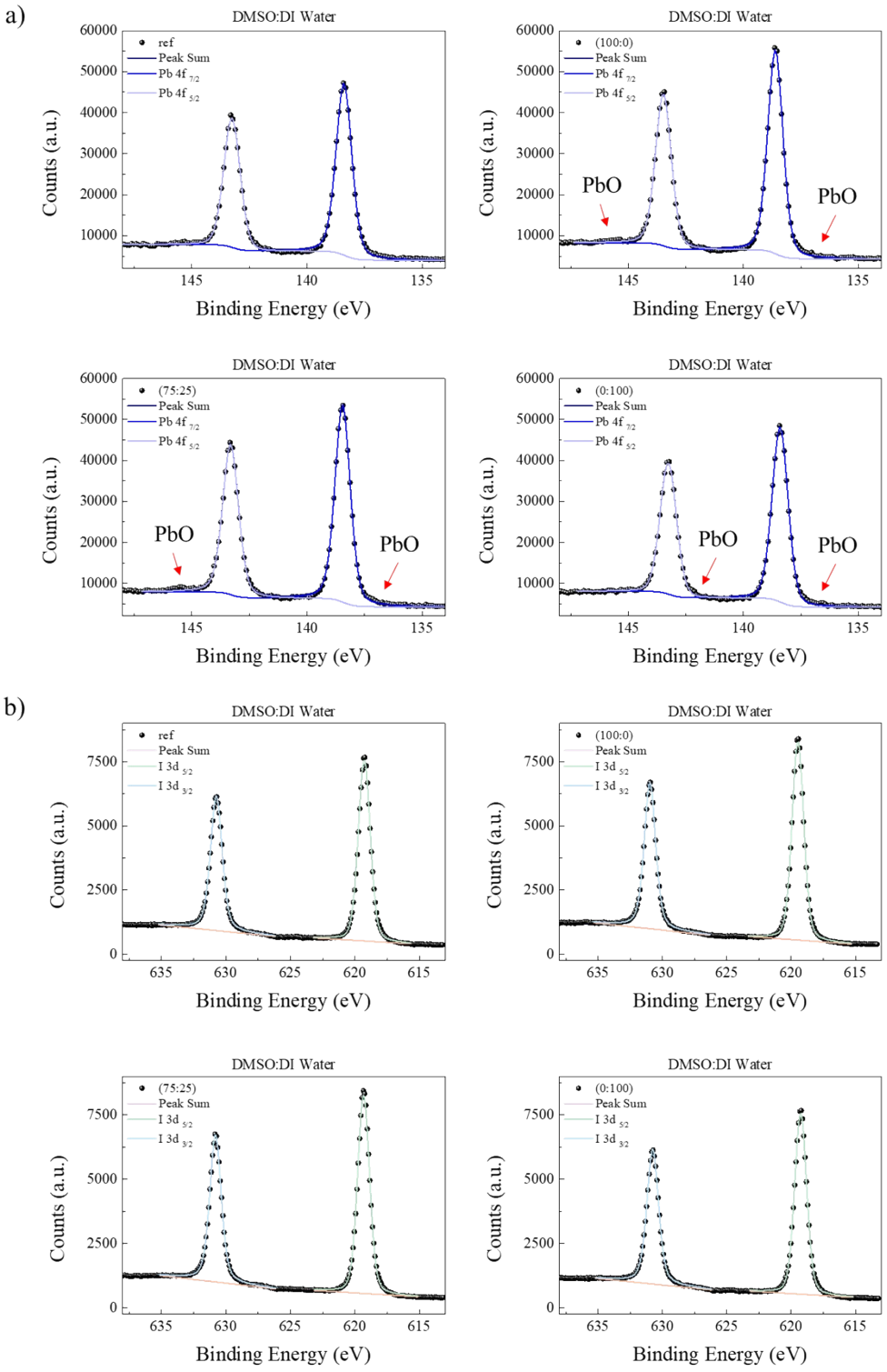

Figure S3 a) XPS spectra and analyses of the SVA-processed perovskite films a) Pb 4f b) I 3d.

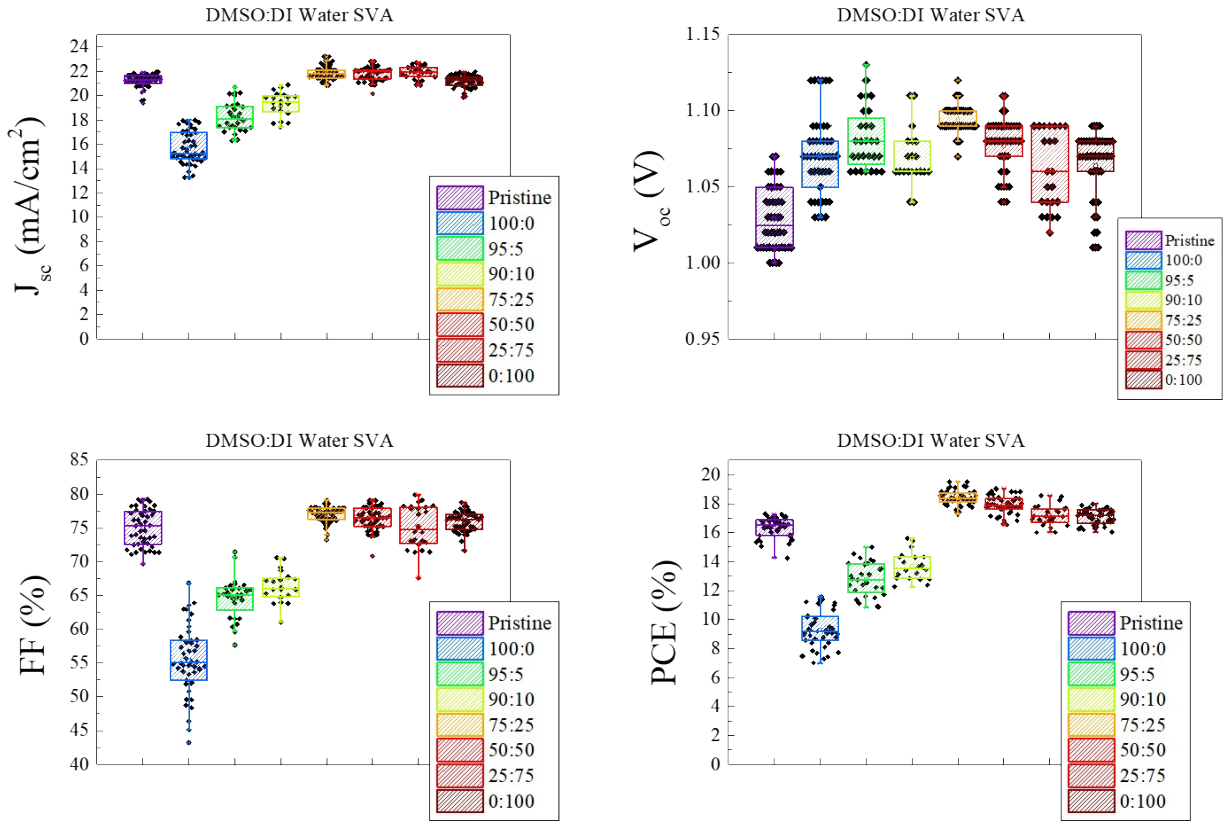

Figure S4 The statistical graphs displaying the device efficiency of more than 50 cells as a function of the DMSO:DI water ratio during the SVA process.

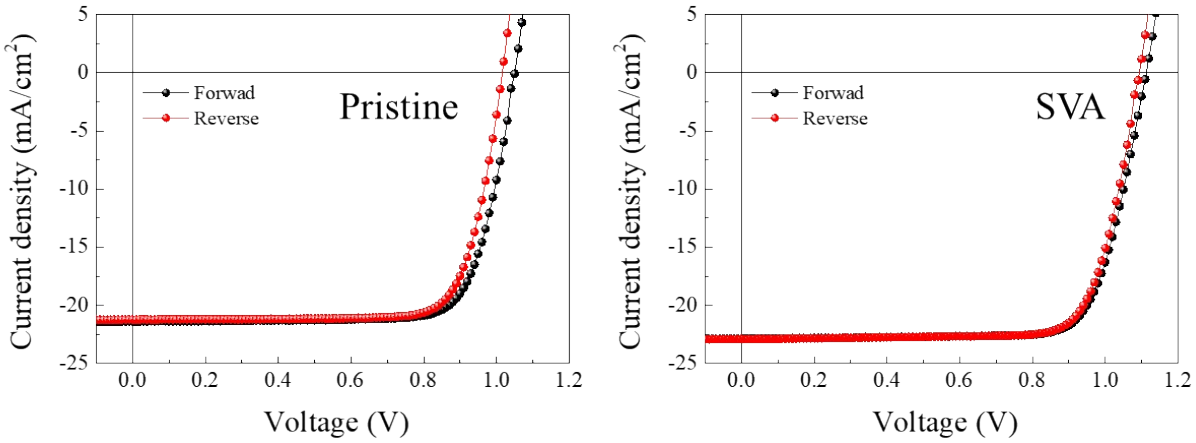

Figure S5 The instantaneous J-V curves of the perovskite solar cells with definite hysteresis. The black line indicates a forward scan and the red line is the reverse scan. The J-V curve of the SVA-processed device shows negligible hysteresis and similar photovoltaic parameters regardless of the scan direction.

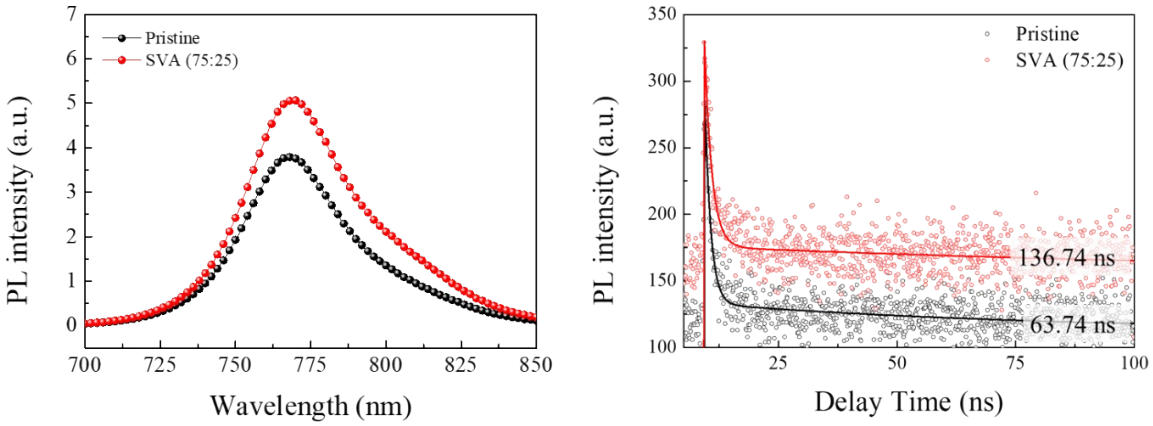

Figure S6 Photoluminescence (PL) spectra and time-resolved PL (TRPL) spectra of the pristine and SVA-processed perovskite films.

	τ_{avg}	A_1	Proportion (%)	τ_1 (ns)	A_2	Proportion (%)	τ_2 (ns)
Pristine	63.738	164.996	88.69	1.242	21.031	11.31	72.175
SVA	136.737	164.354	87.87	1.556	22.689	12.13	147.10

For, TRPL analysis, the curves were fitted using a bi-exponential decay model ($y = A_1\exp[-(x–x0)/\tau_1] + A_2(\exp[-(x–x0)/\tau_2])$, and the fitted parameters are summarized in Table.

First, the steady-state photoluminescence (PL) results showed that the intensity of SVA-treated thin films is higher than that of pristine. This result indicated that SVA treatment was effective for reducing grain density and grain boundaries passivation in perovskite films which was also consistent with time-resolved PL (TRPL). The SVA films showed both prolonged τ_1 (due to charge carrier trapping defect) and τ_2 (due to bimolecular radiative recombination in the bulk crystals). In particular, τ_2 increased by more than about two times, indicating that the bulk carrier life is longer due to the much larger grain size, improved perovskite crystallinity and preferred orientation with SVA treatment.

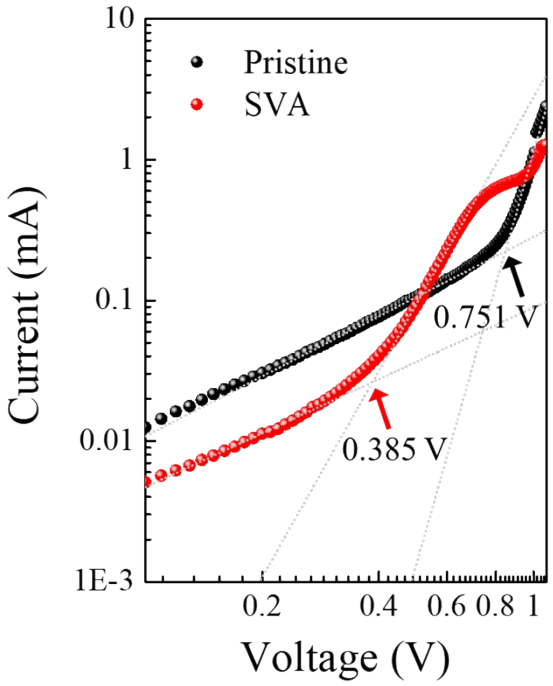

Figure S7 The dark I–V curves of the pristine and SVA-processed device revealing the V_{TFL} kink point behavior.

We also conducted the space charge limited current (SCLC) examinations with a structure of ITO / NiOx / Perovskite / Au to assess the trap density in the films. As shown in Figure below, the devices exhibit ohmic response (linear relation) at low bias and a marked increase of the current injection at the intermediate region since the traps are continuously filled with increasing bias until reaching the trap-filling limit voltage (V_{TFL}). And the defects density is calculated from the V_{TFL} based on Equation (1) [1-2]

$$n_t = \frac{2\varepsilon\varepsilon_0 V_{TFL}}{eL^2} \qquad (1)$$

where ε is the relative dielectric constant of perovskite, ε_0 is the vacuum permittivity, e is the electron charge, and L is the thickness of perovskite film.

The calculated values indicate that the Pristine thin film was 7.90×10^{15} cm^{-3} and the SVA thin film was 4.05×10^{15} cm^{-3}, which revealed the reduced trap density by about two times than that of the pristine.

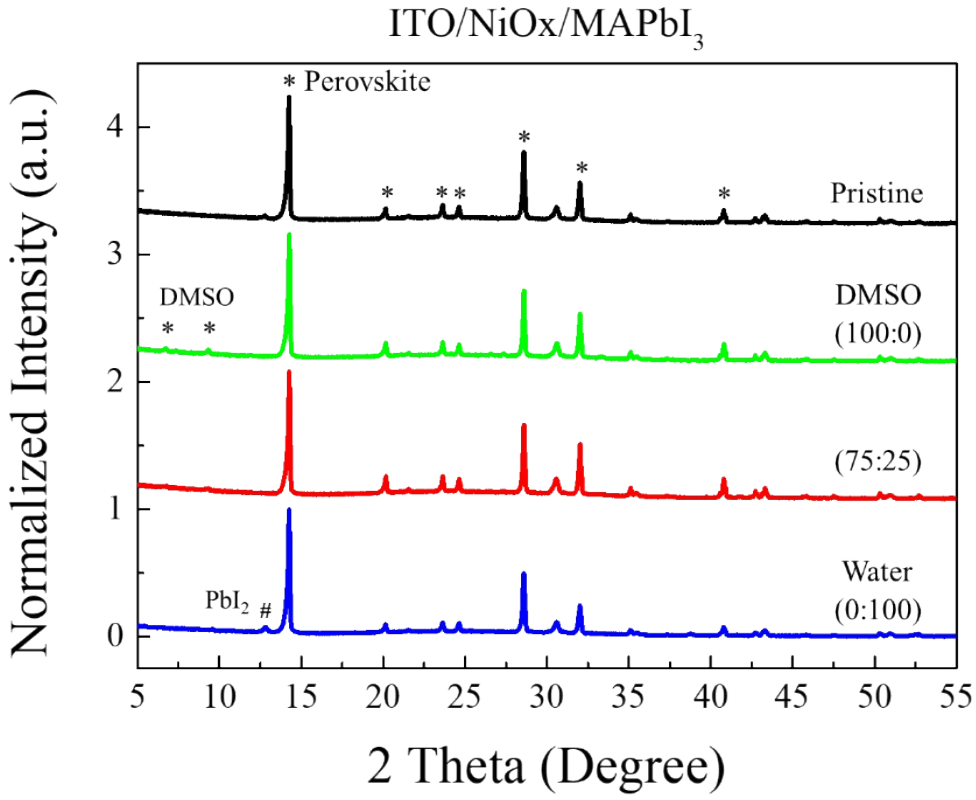

Figure S8 X-ray diffraction spectra of the pristine and SVA-processed $MAPbI_3$ films.

Table S 1 The detailed information of C 1s spectra.

$MAPbI_3$	C 1s	O=C-OH	O-C-O/O-C=O	C-O-C/C=O	CH3-NH3+	CH3-NH2	C-OH	C-C/C-H	intermediate
ref	B.E (eV)				286.88	286.48	285.27	284.80	284.37
	Intensity (a.u.)				4093.53	6250.34	1188.08	1748.67	408.11
	FWHM (eV)				1.358	0.876	0.766	0.913	0.656
	Percentage (%)				29.90%	45.66%	8.68%	12.77%	2.98%
(100:0)	B.E (eV)	289.63		287.33	286.68	286.32	285.24	284.80	284.36
	Intensity (a.u.)	1176.27		719.42	3338.61	4872.89	2045.45	1438.85	1194.95
	FWHM (eV)	2.926		1.125	0.964	0.815	0.803	0.474	0.666
	Percentage (%)	7.96%		4.87%	22.58%	32.96%	13.83%	9.73%	8.08%
(75:25)	B.E (eV)		288.24	287.49	286.70	286.23	285.50	284.80	284.24
	Intensity (a.u.)		830.27	539.57	3305.50	3833.41	1521.50	2451.18	1151.08
	FWHM (eV)		1.516	0.557	0.904	0.684	0.836	0.838	0.732
	Percentage (%)		6.09%	3.96%	24.25%	28.12%	11.16%	17.98%	8.44%
(0:100)	B.E (eV)	289.16			286.79	286.29	285.30	284.80	284.28
	Intensity (a.u.)	359.71			3940.80	5235.25	907.39	1504.32	1223.04
	FWHM (eV)	0.539			1.544	0.898	0.539	0.642	0.772
	Percentage (%)	2.73%			29.92%	39.75%	6.89%	11.42%	9.29%

Table S 2 The detailed information of N 1s spectra.

$MAPbI_3$	N 1s	N-C=O	CH3-NH3+	CH3-NH2	R-NH2
ref	B.E (eV)	403.62	402.71	402.20	401.72
	Intensity (a.u.)	73.44	2971.86	3362.40	703.69
	FWHM (eV)	0.404	0.916	0.823	0.975
	Percentage (%)	0.93%	41.79%	47.38%	9.90%
(100:0)	B.E (eV)	403.33	402.69	402.23	401.65
	Intensity (a.u.)	335.16	3068.18	2544.84	159.42
	FWHM (eV)	0.724	0.865	0.83	0.494
	Percentage (%)	5.49%	50.24%	41.67%	2.61%
(75:25)	B.E (eV)	403.10	402.51	402.11	401.42
	Intensity (a.u.)	377.36	3459.12	2225.70	157.23
	FWHM (eV)	0.765	0.961	0.855	0.498
	Percentage (%)	6.07%	55.62%	35.79%	2.53%
(0:100)	B.E (eV)	403.20	402.59	402.11	401.28
	Intensity (a.u.)	599.26	3723.88	2571.40	94.04
	FWHM (eV)	0.979	0.912	0.835	0.402
	Percentage (%)	8.57%	53.29%	36.79%	1.35%

Table S 3 The detailed information of O 1s spectra.

$MAPbI_3$	O 1s	H2O	O=C-N	O=C-OH	O=C-O	O-C-O	C=O	C-O	intermediate
ref	B.E (eV)		534.76		533.77		532.67		531.80
	Intensity (a.u.)		55.50		293.43		286.06		46.43
	FWHM (eV)		0.650		1.055		1.279		0.592
	Percentage (%)		8.14%		43.06%		41.98%		6.81%
(100:0)	B.E (eV)		534.92	534.26	533.57		532.67		531.83
	Intensity (a.u.)		102.56	69.63	422.13		362.21		140.91
	FWHM (eV)		1.476	0.312	1.007		0.862		0.696
	Percentage (%)		9.35%	6.35%	38.46%		33.01%		12.84%
(75:25)	B.E (eV)	536.06	534.46		533.63	533.03		532.49	531.76
	Intensity (a.u.)	88.22	92.60		169.45	307.22		197.78	74.77
	FWHM (eV)	1.569	0.680		0.668	0.558		0.666	0.401
	Percentage (%)	9.49%	9.96%		18.22%	33.03%		21.27%	8.04%
(0:100)	B.E (eV)	535.95	534.45	533.92		533.16		532.48	531.90
	Intensity (a.u.)	128.21	102.56	141.03		331.92		192.31	97.84
	FWHM (eV)	1.063	0.730	0.748		0.920		0.485	0.614
	Percentage (%)	12.90%	10.32%	14.19%		33.40%		19.35%	9.84%

Reference

(1) Adv. Energy Mater. 2019, 1901852

(2) Energy Environ. Sci., 2018,11, 3349-3357